BIOCHEMISTRY
including biophysical chemistry & molecular biology

Article

pubs.acs.org/biochemistry

Interaction of 14-3-3ζ with Microtubule-Associated Protein Tau within Alzheimer's Disease Neurofibrillary Tangles

Hamid Y. Qureshi,[†] Tong Li,[†] Ryen MacDonald,[†,‡] Chul Min Cho,[†,‡] Nicole Leclerc,[§] and Hemant K. Paudel*[,†,‡]

[†]The Bloomfield Center for Research in Aging, Lady Davis Institute for Medical Research, Jewish General Hospital, 3755 Côte-Sainte-Catherine Road, Montreal, Quebec, Canada H3T 1E2

[‡]Department of Neurology and Neurosurgery, McGill University, Montreal, Quebec, Canada H3A 0G4

[§]Department of Pathology, University of Montreal, Montreal, Quebec, Canada H3T 1E2

Supporting Information

ABSTRACT: Alzheimer's disease (AD) is characterized by the presence of abnormal, straight filaments and paired helical filaments (PHFs) that are coated with amorphous aggregates. When PHFs are treated with alkali, they untwist and form filaments with a ribbonlike morphology. Tau protein is the major component of all of these ultrastructures. 14-3-3ζ is present in NFTs and is significantly upregulated in AD brain. The molecular basis of the association of 14-3-3ζ within NFTs and the pathological significance of its association are not known. In this study, we have found that 14-3-3ζ is copurified and co-immunoprecipitates with tau from NFTs of AD brain extract. *In vitro*, tau binds to both phosphorylated and nonphosphorylated tau. When incubated with 14-3-3ζ, tau forms amorphous aggregates, single-stranded, straight filaments, ribbonlike filaments, and PHF-like filaments, all of which resemble the corresponding ultrastructures found in AD brain. Immuno-electron microscopy determined that both tau and 14-3-3ζ are present in these ultrastructures and that they are formed in an incubation time-dependent manner. Amorphous aggregates are formed first. As the incubation time increases, the size of amorphous aggregates increases and they are incorporated into single-stranded filaments. Single-stranded filaments laterally associate to form double-stranded, ribbonlike, and PHF-like filaments. Both tau and phosphorylated tau aggregate in a similar manner when they are incubated with 14-3-3ζ. Our data suggest that 14-3-3ζ has a role in the fibrillization of tau in AD brain, and that tau phosphorylation does not affect 14-3-3ζ-induced tau aggregation.

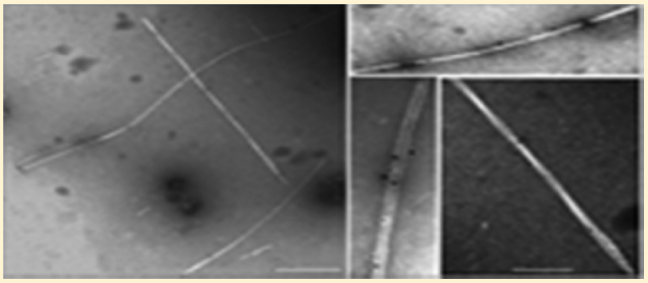

Senile plaques and neurofibrillary tangles (NFTs) are the two characteristic neuropathological lesions found in the brains of patients suffering from AD.[1,2] Electron microscopy (EM) studies have shown that NFTs are composed mainly of paired helical filaments (PHFs) along with a small population of straight filaments.[3,4] Straight filaments are single-stranded and have an average width of 15 nm, which remains constant throughout the length of the filament.[3] PHFs, on the other hand, are composed of two filaments wrapped around each other forming a helical structure.[4,5] The longitudinal spacing between the crossover of two filaments was found to be ∼80 nm and the width to be 10−15 and 27−34 nm in the narrow and wide regions, respectively.[4,5] When PHFs are treated with alkali, they unwind. The unwound filaments display a greater periodicity than PHFs as well as a ribbonlike morphology.[4] When isolated from autopsied brain homogenate, both straight filaments and PHFs contain a fuzzy outer coat that can be removed by proteinase digestion.[3,6,7] Hyperphosphorylated, microtubule-associated protein tau is the major structural component of PHFs, straight filaments, and the fuzzy coat surrounding these filaments.[2,3] *In vitro*, hyperphosphorylation does not cause tau aggregation. It is not known how tau forms these various morphological structures in AD brain.

14-3-3 is a small protein that regulates a wide variety of physiological processes. There are seven different genes that encode highly conserved 14-3-3 isoforms β, γ, ε, τ, η, σ, and ζ (α and δ are phosphorylated forms of β and ζ, respectively).[8] An earlier study by Layfield et al. reported the presence of 14-3-3 in NFTs of AD brains.[9] Later, Umehara et al. reported that only the 14-3-3ζ isoform was associated with NFTs.[10] When Soulie et al. examined various stress-related genes in AD brain, they found that, of 236 genes analyzed, the expression of 14-3-3ζ was upregulated most significantly.[11] A profound increase in the level of 14-3-3ζ expression was seen in the areas affected by NFTs. This study showed that 14-3-3ζ upregulation is an early event and correlates with the severity of AD pathology.[11] Recently, a number of studies have shown that 14-3-3ζ binds to tau and promotes tau phosphorylation and aggregation *in*

Received: April 8, 2013
Revised: August 19, 2013
Published: August 20, 2013

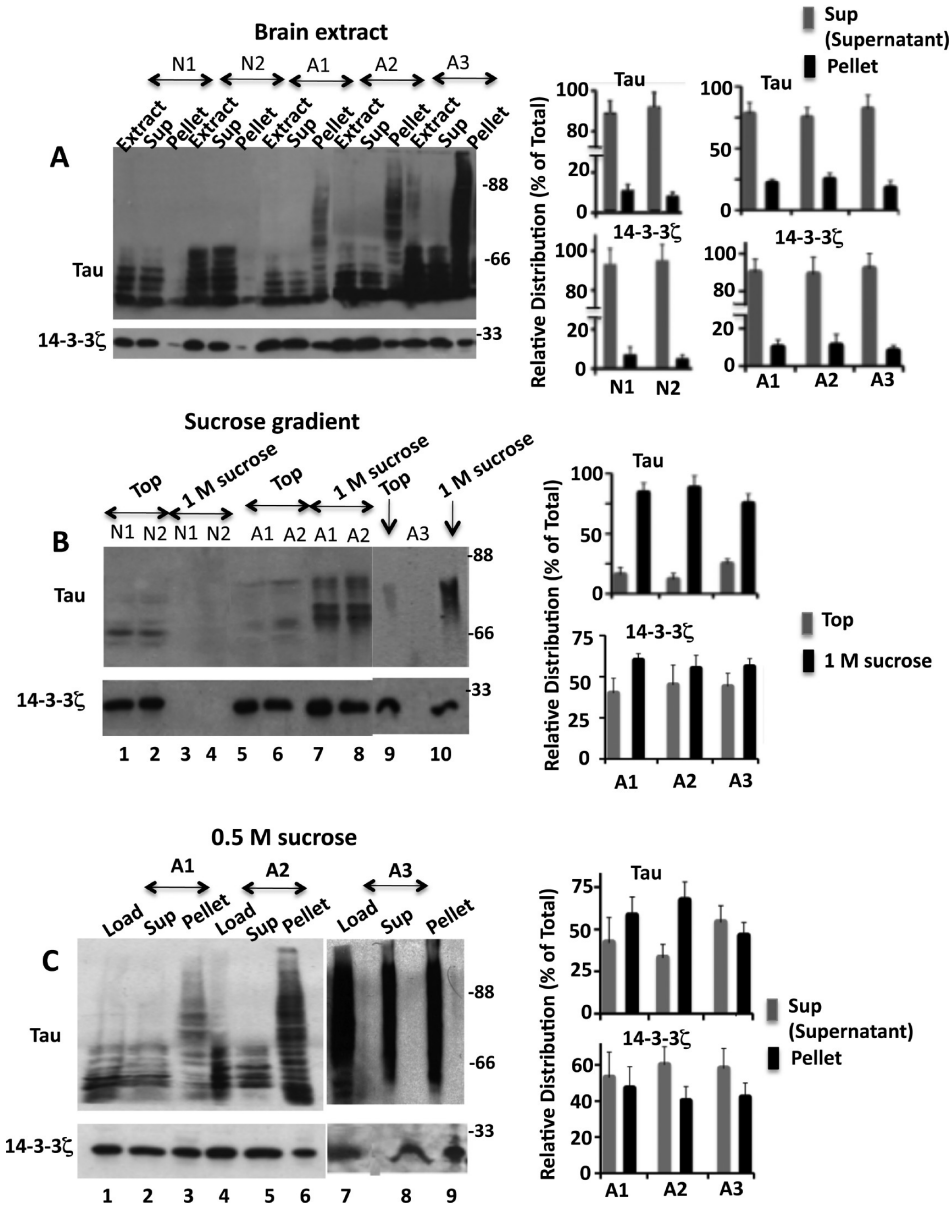

Figure 1. 14-3-3ζ is copurified with PHFs from AD brain extract. PHFs were partially purified from brain extracts by discontinuous sucrose density gradient centrifugation. Various fractions were subjected to Western blot analysis using anti-tau or anti-14-3-3ζ antibodies. On the basis of blot band intensities, relative amounts of tau and 14-3-3ζ in various fractions were calculated. (A) Western blot analysis of brain extract. (B) Western blot analysis of sucrose density gradient fractions. (C) Western blot analysis of 0.5 M sucrose gradient centrifugation fractions. Values in the bar graphs are means ± SE from three Western blots of each sample.

vitro.[12−21] The pathophysiological significance of these observations remains undetermined.

In this study, we have investigated the interaction of 14-3-3ζ with tau in AD brain extract and *in vitro*. Herein, we report that 14-3-3ζ co-immunoprecipitates with tau from the partially purified NFTs of AD brain. Using EM, we show that when tau is incubated with 14-3-3ζ, it forms amorphous aggregates, single-stranded filaments, double-stranded filaments, ribbonlike filaments, and PHF-like filaments in a time-dependent manner. We also demonstrate that both tau and phosphorylated tau aggregate in a similar manner. Our data show that tau phosphorylation does not affect 14-3-3ζ-induced tau fibrillization *in vitro*.

MATERIALS AND METHODS

Partial Purification of PHFs from Human Brain. Tissues from three histopathologically confirmed human AD brains containing abundant tangles and plaques in the frontal and temporal cortex (A1−A3) and two normal age-matched controls (N1 and N2) used in this study were obtained from the University of California (Irvine, CA) and were gifts from H. Schipper of the Lady Davis Institute for Medical Research. PHFs from AD brain cortex were purified as described previously at 4 °C.[22] Each brain was homogenized in an equal amount (w/v) of cold extraction buffer (25 mM Hepes, 1 mM EDTA, 1 mM DTT, and 0.1 M NaCl) supplemented with protease inhibitor cocktail (Roche Scientific) and centrifuged at 27000*g* for 30 min to remove the tissue debris. The supernatant was centrifuged at 100000*g* for 1 h. The pellet was resuspended

dx.doi.org/10.1021/bi400442d | *Biochemistry* 2013, 52, 6445−6455

in extraction buffer containing 0.1% sarkosyl and incubated at 30 °C for 30 min while being shaken constantly. The suspension was loaded onto a discontinuous sucrose gradient (0.1 and 1.5 M) in extraction buffer and centrifuged at 100000*g* for 1 h. Various fractions were collected, and the 1 M fraction containing PHFs was loaded onto a 0.5 M sucrose solution in extraction buffer and centrifuged at 100000*g* for 1 h. The supernatant and pellet were separated and subjected to Western blot analysis.

Proteins and Antibodies. Tau was purified from bacterial extract expressing the longest isoform of human tau, as described previously.[23] GST-14-3-3ζ and GST were purified from bacterial extracts using glutathione Sepharose affinity chromatography equilibrated in Hepes buffer [25 mM Hepes (pH 7.2), 0.2 mM EDTA, and 0.1 mM DTT] supplemented with protease inhibitor cocktail.[14] Purified GST-14-3-3ζ was treated with precision protease to separate GST and 14-3-3ζ. The treated sample was chromatographed through a glutathione Sepharose column. Effluent fractions containing 14-3-3ζ were collected and dialyzed against Hepes buffer. Monoclonal anti-14-3-3ζ and anti-tau antibodies were obtained from Zymed Laboratories. Monoclonal anti-HA, ant-Myc, and anti-Flag were obtained from Sigma. A polyclonal anti-tau antibody was a gift from J. Wang (University of Calgary, Calgary, AB).[14]

Protein Concentrations. The concentration of tau was determined by a spectrophotometer, as described previously.[23] The concentration of phosphorylated tau was determined by the Bio-Rad protein assay using tau as the standard. Concentrations of 14-3-3ζ and GST were determined using the Bio-Rad protein assay with BSA as the standard.

Preparation of Phosphorylated Tau. The recombinant longest human tau isoform was purified from lysates of *Escherichia coli* bacteria as described previously.[23] Purified tau was phosphorylated via incubation with a fresh rat brain extract, as described previously.[24] The final concentrations of the various components in the mixture were as follows: 1 mg/mL tau, 25 mM Hepes (pH 7.2), 0.1 mM EDTA, 0.1 mM DTT, 10 mM NaF, 50 mM β-glycerol phosphate, 0.5 mM [γ-^{32}P]ATP, 10 mM $MgCl_2$, 0.1 mM $CaCl_2$, phosphatase, and protease inhibitor cocktail (Roche Scientific), and carryover amounts of brain extract. Incubation at 30 °C for 4 h resulted in the incorporation of 7.9 mol of phosphate/mol of tau as determined by a filter paper assay.[23] The vial containing the reaction mixture was placed into a boiling water bath followed by centrifugation. The supernatant containing heat stable phosphorylated tau was withdrawn, desalted on a Sephadex G25 column, and stored at −80 °C until it was used.

Quantitative Sedimentation Assay of Tau Aggregation. Tau aggregation was monitored and quantified by a method previously described by Giasson et al.[25] Tau (0.5 mg/mL) was mixed with 14-3-3ζ (0.2 mg/mL), GST (0.2 mg/mL), or heparin (0.1 mg/mL) in 20 mM MOPS containing protease inhibitor cocktail and incubated for 96 h at 37 °C. After incubation, the samples were centrifuged at 100000*g* for 1 h. The supernatant and pellet were separated and subjected to Western blot analysis. On the basis of blot band intensities, the relative amount of each protein in the pellet and the supernatant was calculated. The relative amount of protein in the pellet was regarded as the aggregated protein and expressed as the percentage of the total (amount in the pellet plus that in the supernatant).

Immunoprecipitation and GST Pull-Down Assay. Immunoprecipitation of Flag-tau and Myc-14-3-3ζ from the HEK-293 cell extract was performed as described previously.[26] To immunoprecipitate tau or 14-3-3ζ from PHFs, 110 μL of the 1 M sucrose fraction of the PHF preparation from Figure 1 was precleared with 30 μL of protein G agarose beads equilibrated in extraction buffer. To 50 μL of precleared sample was added 10 μL of nonspecific serum, anti-tau, or anti-14-3-3ζ antibody. All samples were incubated with end-over-end shaking at 4 °C. After the sample had been shaken for 12 h, 25 μL of protein G agarose beads pre-equilibrated in extraction buffer was added to each sample, and incubation and shaking were continued. After 5 h, samples were centrifuged, and the recovered beads were washed three times, dissolved in 30 μL of sodium dodecyl sulfate−polyacrylamide gel electrophoresis (SDS−PAGE) sample buffer, boiled, and subjected to Western blot analysis. The procedure for the GST pull-down assay has been described previously.[26]

EM. Tau (0.5 mg/mL) was mixed with 14-3-3ζ (0.2 mg/mL), GST (0.2 mg/mL), or heparin (0.1 mg/mL) and incubated for various amounts of time in aggregation buffer [20 mM MOPS (pH 7.0)]. At each time point, samples were placed on a 300 mesh carbon-coated copper grid and incubated for 5 min to allow the samples to be absorbed. The grids were then washed five times with PBS and blocked with 2% BSA in PBS for 30 min. After the sample had been blocked, the anti-tau polyclonal antibody in a BSA/PBS mixture was added to each grid and the incubation was continued. After 1 h, grids were washed with a BSA/PBS mixture five times and then incubated with anti-14-3-3ζ monoclonal antibody in a BSA/PBS mixture for 1 h. After five washes, the grids were sequentially labeled with anti-rabbit followed by anti-mouse secondary antibodies conjugated to 10 and 18 nm colloidal gold, respectively. After being labeled, the grids were washed with PBS five times, negatively stained with 1% urinyl acetate for 1 min, and viewed with an electron microscope.

RESULTS

14-3-3ζ Is Copurified with PHFs from Autopsied AD Brain. When autopsied normal human brain homogenates (N1 and N2) were centrifuged, 11 and 8% of the total tau, respectively, were present in the pellet containing insoluble materials (Figure 1A). On the other hand, in AD brain homogenates A1−A3, 22, 25, and 18% of the total tau, respectively, remained in the pellet. When analyzed for 14-3-3ζ, N1 and N2 samples had 7 and 5% of the total in the pellet and A1−A3 contained 10, 11, and 8% of the total in the pellet, respectively. Thus, AD brains contain more of both insoluble tau and 14-3-3ζ than normal brains. However, while the relative amounts of tau and 14-3-3ζ that were recovered in the pellets of normal brain were similar, AD brain displayed larger relative amounts of insoluble tau than 14-3-3ζ.

When various pellets from the fractionations described above were suspended in detergent and subjected to a discontinuous sucrose density centrifugation, almost all of the tau and 14-3-3ζ from each of the normal N1 and N2 brain samples were present in the top layer containing soluble proteins (Figure 1B, lanes 1 and 2, respectively). These data showed that most of the tau and 14-3-3ζ in the pellets of normal brains were detergent soluble. When detergent-suspended pellets of AD brain samples were analyzed, 84, 88, and 75% of the total tau from each of the A1, A2, and A3 samples, respectively, that were loaded onto the gradient were present in the 1 M sucrose fraction containing insoluble proteins (Figure 1B, lanes 7, 8, and 10, respectively). When 14-3-3ζ was analyzed, each of the A1, A2, and A3

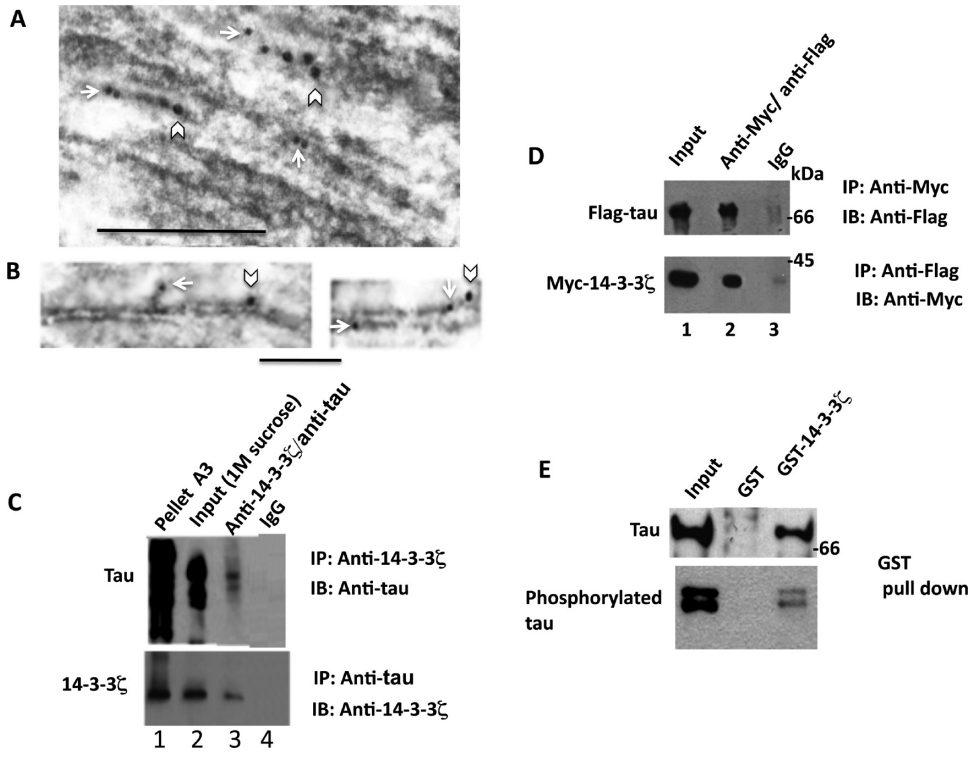

Figure 2. 14-3-3ζ is bound to tau within PHFs. (A and B) Tau and 14-3-3ζ colocalize within PHFs. Partially purified PHF (1 M fraction) was immunogold-labeled with 10 nm anti-tau (arrow) and 18 nm anti-14-3-3ζ (arrowhead) gold particles, negatively stained, and viewed via EM. The scale bar is 200 nm. (C) Partially purified PHF fraction subjected to immunoprecipitation and analyzed by Western blotting. (D) 14-3-3ζ binds to tau in intact cells. HEK-293 cells cotransfected with Flag-tau and Myc-14-3-3ζ were subjected to co-immunoprecipitation using indicated antibodies. IP indicates immunoprecipitation; IB indicates immunoblot. (E) 14-3-3ζ directly binds to tau and phosphorylated tau *in vitro* a GST pull-down assay. Tau or phosphorylated tau (0.1 mg/mL each) in Hepes buffer was pulled down with glutathione Sepharose beads coated with GST-14-3-3ζ and analyzed by Western blot analysis.

samples displayed 60, 55, and 56%, respectively, of the total that was loaded onto the gradient in the 1 M sucrose fraction. Thus, while tau in the pellet of each of the AD brains was mostly insoluble, almost half of 14-3-3ζ was detergent soluble. These data indicate that, compared to the relative amount of insoluble tau, the relative amount of insoluble 14-3-3ζ in AD brain is significantly smaller. When each of the 1 M sucrose fractions was layered atop 0.5 M sucrose and subjected to ultracentrifugation, 58, 67, and 46% of the total tau was present in the pellet, respectively (Figure 1C, lanes 3, 6, and 9, respectively). Similarly, 47, 40, and 42% of the total 14-3-3ζ that was loaded was recovered in the pellets of A1, A2, and A3, respectively. These data show that the relative amounts of both tau and 14-3-3ζ are distributed similarly in the supernatant and pellets of 0.5 M sucrose fractions. Taken together, these data show that 14-3-3ζ remains associated with partially purified PHFs from AD brain.

14-3-3ζ Is Bound to Tau in PHFs. To further evaluate the pathological significance of the presence of 14-3-3ζ in PHFs isolated from AD brain, we asked if 14-3-3ζ is bound to tau within the PHFs. We first examined the 1 M sucrose fraction of AD brain by immunoelectron microscopy (EM). A number of filamentous structures that were co-immunogold-labeled with anti-tau (arrow) and anti-14-3-3ζ (arrowhead) were seen (Figure 2A,B). To substantiate the EM data, we performed a co-immunoprecipitation experiment of 1 M sucrose fractionation. As shown in Figure 2C, tau co-immunoprecipitated with 14-3-3ζ (lane 3) but not IgG (lane 4). Likewise, 14-3-3ζ was pulled down with anti-tau antibody (lane 3). These data indicate that 14-3-3ζ is bound to tau within the PHFs of AD brain.

14-3-3ζ is a phosphoserine-binding protein. However, in many instances, 14-3-3ζ binding is also phosphorylation-independent.[8] PHF-bound tau is hyperphosphorylated.[27] To determine if 14-3-3ζ binds tau within PHFs because tau is phosphorylated, we characterized the interaction of tau with 14-3-3ζ. We cotransfected Flag-tau and Myc-14-3-3ζ into HEK-293 cells. Transfected cells were lysed and subjected to co-immunoprecipitation using anti-Flag and anti-Myc antibodies. Myc-14-3-3ζ co-immunoprecipitated with Flag-tau and vice versa (Figure 2D, lane 2). These data confirm the previous report[14] and show that 14-3-3ζ binds to tau in intact cells and does not require any neuron-specific factors for binding.

To determine if tau phosphorylation is required for 14-3-3ζ–tau binding and if 14-3-3ζ can directly bind to tau, we mixed bacterially expressed nonphosphorylated or phosphorylated tau with glutathione Sepharose beads coated with GST-14-3-3ζ or control GST in a binding mixture. Each mixture was centrifuged, and the beads were analyzed. Tau was specifically pulled down with GST-14-3-3ζ but not with GST (Figure 2E). Likewise, phosphorylated tau came down with GST-14-3-3ζ but not GST. These data are consistent with the previous report[14] and indicate that 14-3-3ζ directly binds to both nonphosphorylated and phosphorylated tau.

14-3-3ζ Promotes Tau Aggregation *in Vitro*. Despite being a highly soluble protein, tau aggregates in AD brain. The cause is not known. To determine if 14-3-3ζ has any role, we incubated tau with 14-3-3ζ. Tau incubated with GST, heparin,

or Hepes buffer was used as a control. Both GST and 14-3-3ζ used in this study were bacterially expressed, recombinant proteins that were purified using glutathione Sepharose affinity chromatography from their respective bacterial lysates. In addition, both GST and 14-3-3ζ have similar sizes, running as 25 and 28 kDa bands on an SDS gel, respectively. Therefore, GST was used as a nonspecific control against 14-3-3ζ. Heparin has been widely used to induce tau aggregation *in vitro* at neutral pH.[28,29] Therefore, heparin was used as the positive control. 14-3-3ζ was purified and stored in Hepes buffer. The Hepes buffer was used to investigate if tau aggregation is caused by any components of the buffer containing 14-3-3ζ or tau aggregates in the absence of any cofactor. After 96 h at 37 °C, samples were subjected to a quantitative sedimentation assay. The supernatant containing the soluble fraction and the pellet containing the insoluble materials were subjected to SDS−PAGE and Western blot analysis.

SDS−PAGE analysis showed that the relative amount of tau in the pellet of a sample containing tau and Hepes buffer was 6.3% of the total (Figure 3A, lane 2). Likewise, the relative amount of GST or 14-3-3ζ in the pellet was 5.6 or 6.1% of the total in the samples containing GST or 14-3-3ζ alone, respectively (data not shown). The relative amount of tau in the pellet of a sample containing tau and heparin was 35.4% of the total (Figure 3A, lane 8). Similarly, the relative amount of tau in the pellet of a sample containing tau and 14-3-3ζ was 33.8% of the total (Figure 3A, lane 4). To determine if the tau found in these pellets was a carryover soluble protein trapped in the pellet or if it existed in an aggregated form that settled during centrifugation, each pellet was resuspended in Hepes buffer and incubated at room temperature for 1 h with constant shaking. After incubation, the samples were recentrifuged and analyzed. As shown in Figure 3B, tau from the pellets of the samples containing tau and buffer or tau and GST was dissolved in the buffer during incubation and recovered in the supernatant (lanes 1 and 5). These data showed that a small amount of tau that was detected in the respective pellets of these samples (Figure 3A, lanes 2 and 6) is carryover soluble tau that was trapped in the pellet during centrifugation. In contrast, most of the tau from the pellet of a sample containing tau and heparin did not dissolve in the buffer and remained in the pellet after centrifugation (Figure 3B, lane 8). This result indicated that most of the tau in the pellet of the sample containing heparin existed in an aggregated form. These data are consistent with previous reports[28] and show that tau aggregates when incubated with heparin. More importantly, most of the tau in the pellet of the sample containing 14-3-3ζ and tau also did not dissolve and remained in the pellet (Figure 3B, lane 4). On the basis of these data, we concluded that tau becomes insoluble when incubated with 14-3-3ζ for 96 h.

Effect of Incubation Time on 14-3-3ζ-Induced Tau Aggregation. To further characterize tau aggregation, we incubated a fixed amount of tau with varying amounts of 14-3-3ζ for 96 h. After incubation, each sample was analyzed via a sedimentation assay for aggregation. The percent of tau in the pellet of each sample was regarded as the aggregated tau. As shown in Figure 4A, the relative amount of tau in the pellet of the sample containing only tau was 5.5% of the total. On the basis of the data in Figure 3, this amount was regarded as the basal amount of carryover soluble tau that was trapped in the pellet during centrifugation. The relative amount of tau in the pellet became 12.9% of the total when 14-3-3ζ (0.05 mg/mL) was included in the incubation mixture (Figure 4A, lane 4).

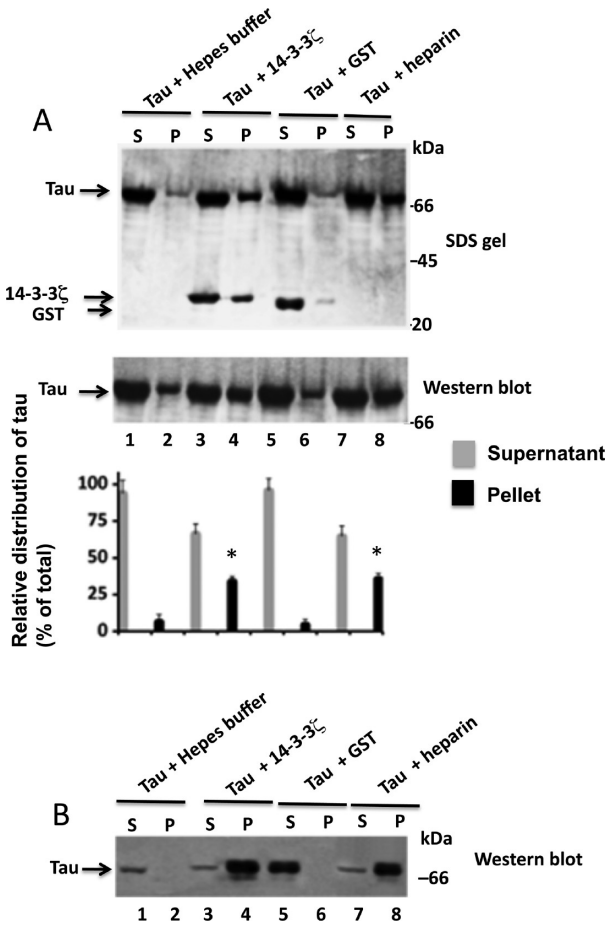

Figure 3. 14-3-3ζ promotes tau aggregation *in vitro*. Tau was mixed with 14-3-3ζ, Hepes buffer, GST, or heparin and incubated at 37 °C for 96 h. After being incubated, each sample was analyzed via a quantitative sedimentation assay. The resulting pellet (P) and the supernatant (S) of each sample were separated. Each pellet was then dispersed in Hepes buffer, incubated with constant shaking, and recentrifuged. The resulting pellet and the supernatant were separated. All fractions were subjected to Western blot analysis. On the basis of blot band intensities, the relative amount of tau in the indicated fractions was calculated. (A) SDS−PAGE and Western blot analysis of pellet and supernatant fractions after centrifugation. The top panel represents a Coomassie Brilliant Blue-stained SDS gel. The middle panel represents a Western blot. The bottom panel is the relative distribution that, in various fractions, was calculated from the top panel representing the protein-stained SDS−PAGE gel. The values with SE are from Western blot analysis of three independent experiments. *$p <$ 0.005 with respect to tau incubated with GST (t test). (B) Western blot of supernatant and pellet fractions obtained after recentrifugation. Similar observations were made in three independent experiments.

This value became 25.9, 32.8, and 36.7% when the level of 14-3-3ζ increased to 0.1, 0.2, and 0.5 mg/mL, respectively (Figure 4A, bottom panel). Thus, with increasing amounts of 14-3-3ζ, more and more tau aggregated.

We then incubated fixed amounts of tau with 14-3-3ζ. At various time points, the samples were analyzed for tau aggregation via a sedimentation assay. As shown in Figure 4B, at time zero, 4.3% of the total tau was present in the pellet, representing the insoluble fraction. At the 24 h time point, the relative amount of tau in the pellet slightly increased and became 8.5% of the total. At the 48 h time point, however, 25.8% of total tau aggregated. Likewise, the relative amount of tau aggregated at the 72 h time point was 30.3% of the total and

dx.doi.org/10.1021/bi400442d | *Biochemistry* 2013, 52, 6445−6455

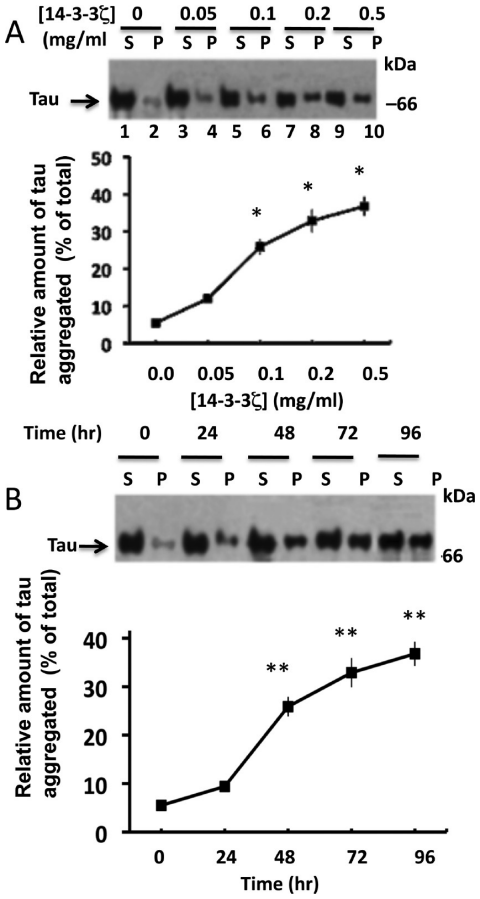

Figure 4. 14-3-3ζ promotes concentration- and time-dependent aggregation of tau. Tau (0.5 mg/mL) was incubated either with increasing amounts of 14-3-3ζ for 96 h or with 0.2 mg/mL 14-3-3ζ for various periods of time. After incubation, samples were analyzed via a quantitative sedimentation assay. On the basis of the blot band intensities, the relative amount of aggregated tau in each sample was calculated. (A) Western blot analysis of tau incubated with various amounts of 14-3-3ζ. (B) Western blot analysis of tau incubated with 0.2 mg/mL 14-3-3ζ for various periods of time. Graphs with SE are based on the respective data from three independent determinations. *$p < 0.05$ with respect to tau incubated with buffer; **$p < 0.01$ with respect to time zero (t test).

at the 96 h time point 34.9% of the total. In summary, incubation of tau with 14-3-3ζ for 24 h did not cause any significant effects, but after 48 h, the level of tau aggregation increased with increasing incubation time.

EM Analyses of Tau Aggregation. In AD, tau aggregates, forming characteristic PHFs, straight filaments, and amorphous ultrastructures. To determine if 14-3-3ζ-induced tau aggregates form any ultrastructures that may resemble those seen in AD brain, we incubated tau and 14-3-3ζ for various amounts of time. Each incubated sample was placed on a copper grid, immunogold-labeled with anti-tau and anti-14-3-3ζ antibodies, negatively stained with urinyl acetate, and viewed by EM. Tau incubated with GST or heparin was used as a control.

None of the samples that were incubated for 24 h showed any visible negatively stained structures under the electron microscope (data not shown). However, at 48 h, while tau incubated with GST did not show any ultrastructure, tau with heparin displayed large structures with a disordered morphology (Figure 1 of the Supporting Information). These amorphous aggregates were immunogold-labeled with anti-tau antibody (arrow), indicating that they represented aggregated tau.

Tau incubated with 14-3-3ζ for 48 h also displayed amorphous aggregates of different sizes that had relatively low contrast under the electron microscope (Figure 5A, arrow). 14-3-3ζ-induced aggregates were heavily labeled with anti-tau antibody (Figure 5B,C, arrow) and a few with anti-14-3-3ζ antibody (Figure 5B,C, arrowhead). When compared, 14-3-3ζ-induced amorphous aggregates were more extensively labeled with anti-tau antibody than the amorphous aggregates formed in the presence of heparin (Figure 1 of the Supporting Information). These data show that tau forms amorphous aggregates when incubated with 14-3-3ζ for 48 h.

After 72 h, while tau containing GST did not show any ultrastructure, that incubated with heparin displayed anti-tau immunogold-labeled single-stranded, straight filaments with a width of 16.6 ± 1.8 nm (n = 10) (Figure 2 of the Supporting Information). When tau incubated with 14-3-3ζ for 72 h was analyzed, large amorphous aggregates that were immunogold-labeled with both anti-tau and anti-14-3-3ζ antibodies were observed (Figure 3 of the Supporting Information and Figure 5D,E). These data indicate that the size of amorphous aggregates had grown larger between the 48 and 72 h incubation periods. In addition, most of these aggregates were attached to single-stranded, straight filaments that had a width of 18.4 ± 1.1 nm (n = 10) (arrow) and were decorated with both anti-tau and anti-14-3-3ζ gold particles (Figure 5D,E). The number and size of amorphous aggregates attached to each filament varied, and the aggregates were usually attached throughout the body of the filament and not at the ends. These aggregates displayed less contrast under the electron microscope than the filaments, providing a fuzzy image around the filament. While the amorphous aggregates were extensively labeled, the straight filaments were decorated not so strongly with both anti-tau and anti-14-3-3ζ gold particles. Thus, tau incubated with 14-3-3ζ for 72 h forms single-stranded filaments containing fuzzy, amorphous aggregates.

At the 96 h time point, tau incubated with GST did not show any aggregation, but that with heparin had single-stranded, straight filaments similar to those seen in corresponding samples after the 72 h incubation period (Figure 4 of the Supporting Information). Tau incubated with 14-3-3ζ, on the other hand, displayed four types of ultrastructures that were immunogold-labeled with both anti-tau and anti-14-3-3ζ antibodies (Figure 6A). These were amorphous aggregates (black arrowhead), straight filaments (black single arrow), ribbonlike filaments (black double arrow), and PHF-like filaments (black triple arrow). Amorphous aggregates were few in number and relatively small in size, but similar to those seen in the 72 h samples. These data indicate that between the 72 and 96 h incubation periods, amorphous aggregates had either disappeared or transformed into another structure. Straight filaments had a width of 19.2 ± 2.1 nm (n = 10) and appeared to be identical to the corresponding filaments that were formed at the 72 h incubation time (Figure 6A,B). However, in contrast to the filaments formed after incubation for 72 h, the straight filaments formed after incubation for 96 h were almost completely devoid of amorphous aggregates.

The ribbonlike filaments had very long [1.5 ± 0.1 μm (n = 10)], flat, ribbonlike loops (Figure 6A, black double arrow) that were interrupted by twists (Figure 6A, white arrow). In the area with a flat morphology, the width was 32.2 ± 2.4 nm (n = 10) (Figure 6C). As the loop began to approach the twisted area,

dx.doi.org/10.1021/bi400442d | Biochemistry 2013, 52, 6445−6455

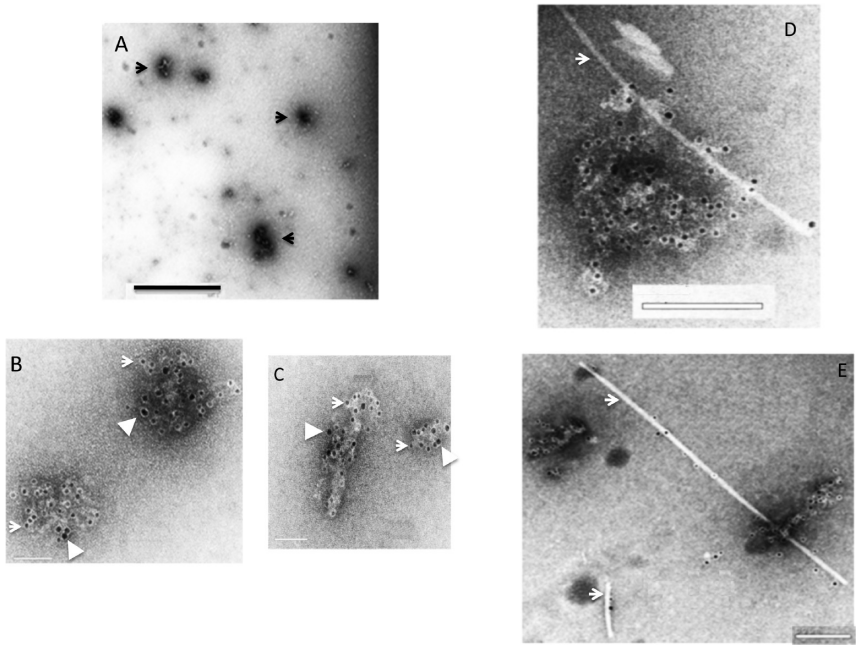

Figure 5. 14-3-3ζ promotes tau fibriilization *in vitro*. (A–C) 14-3-3ζ promotes formation of amorphous tau aggregates at the 48 h incubation time point. Tau mixed with 14-3-3ζ and incubated for 48 h was immunogold-labeled against anti-tau and anti-14-3-3ζ and viewed via EM. (A) Immuno-EM micrograph showing a relatively large field of view. Arrows indicate amorphous aggregates. The scale bar is 500 nm. (B and C) Amorphous aggregates labeled with anti-tau (arrow) and anti-14-3-3ζ (arrowhead) gold particles. Scale bars are 200 nm. (D and E) Tau forms single-stranded straight filaments attached to amorphous aggregates when incubated with 14-3-3ζ for 72 h. Immuno-EM micrographs of single-stranded tau filaments (arrow) formed in the sample containing tau and 14-3-3ζ and incubated for 72 h. Small and large black dots indicate anti-tau and anti-14-3-3ζ gold particles, respectively. Scale bars are 200 nm.

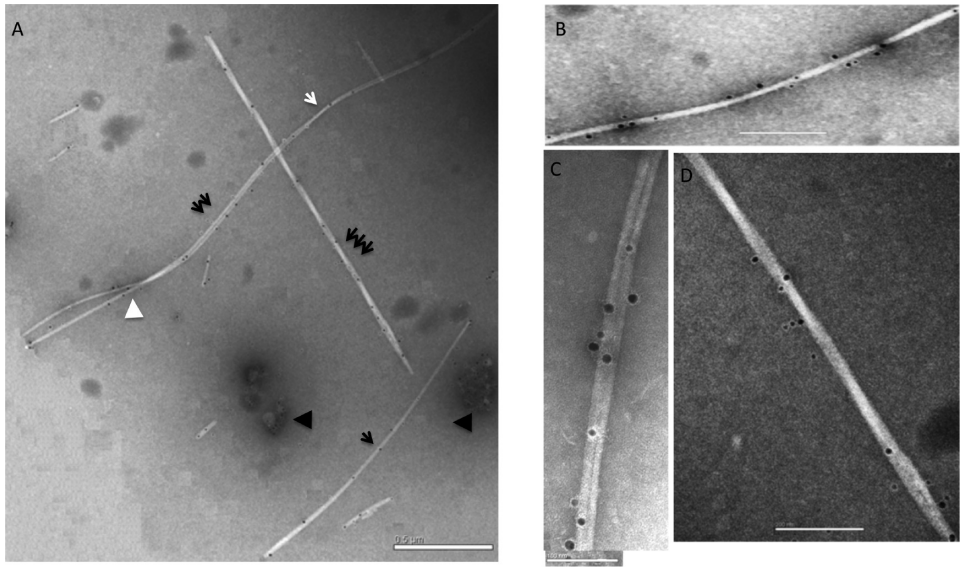

Figure 6. Immuno-EM of tau filaments formed by incubation with 14-3-3ζ for 96 h. Tau mixed with 14-3-3ζ and incubated for 96 h was immunogold-labeled with anti-tau and anti-14-3-3ζ antibodies and viewed under an electron microscope. The small black dots represent the 10 nm gold-labeled anti-tau antibody. The larger black dots represent the 18 nm gold-labeled anti-14-3-3ζ antibody. (A) Large field view. The single, double, and triple black arrows indicate straight filaments, ribbonlike filaments, and PHF-like filaments, respectively. The black arrowhead indicates amorphous aggregates. The white arrow indicates the crossover of the helix, and the white arrowhead indicates the transition point at which the two ribbonlike filaments unzip. The scale bar is 500 nm. (B–D) Immuno-EM of 14-3-3ζ-induced tau filaments at higher magnifications: straight (B), ribbonlike (C), and PHF-like (D) filaments. Small and large black dots represent anti-tau and anti-14-3-3ζ gold particles, respectively. Scale bars are 200 nm (B and D) and 100 nm (C).

the width of the filament gradually decreased until it reached 15 ± 2 nm (n = 10) at the middle of the twist (Figure 6A). Likewise, as the distance from center of the twist increased and it approached the adjacent loop, the width gradually increased to 32.5 nm. Thus, there was a half-periodicity of 1.5 μm. These filaments appeared to be composed of two protofilaments attached laterally with a black line present between them (Figure 6C). The widths of both protofilaments were identical

dx.doi.org/10.1021/bi400442d | *Biochemistry* 2013, 52, 6445–6455

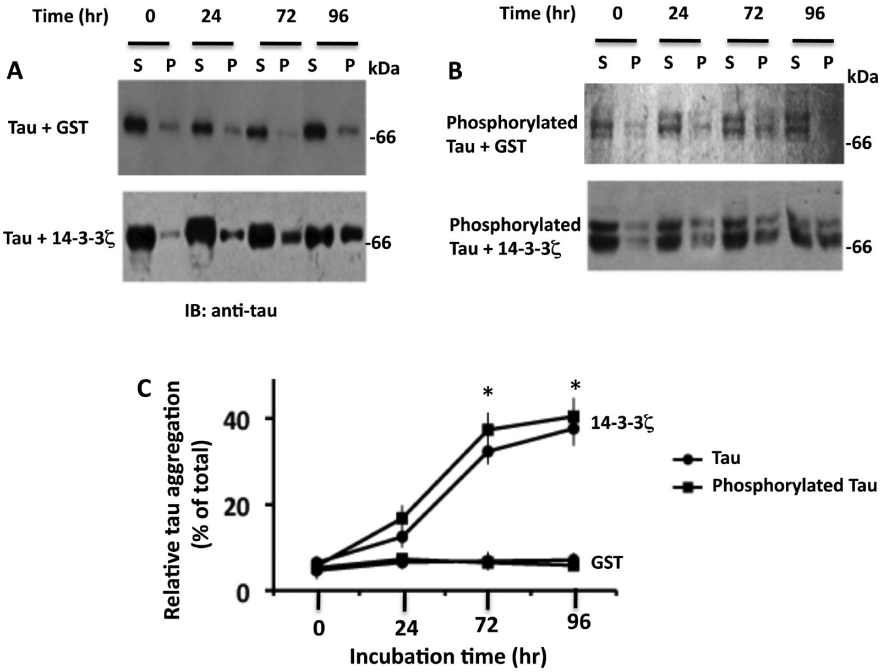

Figure 7. Tau and phosphorylated tau aggregate in the presence of 14-3-3ζ in a similar manner. Tau and phosphorylated tau were individually mixed with GST or 14-3-3ζ and incubated at 37 °C. At various time points, samples were analyzed by a quantitative centrifugation assay for tau aggregation. On the basis of blot analysis, the relative amounts of aggregated tau and aggregated phosphorylated tau were determined. (A) Western blot of tau. (B) Western blot of phosphorylated tau. (C) Relative tau aggregation. Values are means ± SE from respective panels A and B and are averages of three independent determinations. *$p < 0.05$ with respect to incubation time zero (t test).

[14.3 ± 1.1 nm (n = 10)], and both were decorated with anti-tau- and anti-14-3-3ζ-labeled gold particles. Some of the ribbonlike filaments had a sharp transition point at which two straight filaments appeared to unzip from the ribbon (Figure 6A, white arrowhead). These data indicate that the ribbonlike filaments were formed by the lateral association of the two straight filaments. Morphologically, the ribbonlike filaments appeared to be similar to those formed when PHFs of AD brain were treated with alkali.[4]

PHF-like filaments appeared to be composed of two filaments wrapped around each other, giving them a helical morphology (Figure 6A, black triple arrow, and Figure 6D). The length of the spacing between the crossovers was 285 ± 30 nm (n = 10). The width of the filament was 27.9 ± 2.1 nm (n = 10) in the widest loop region and 17.1 ± 2.1 nm (n = 10) in the crossovers. Both protofilaments were decorated with anti-tau- and anti-14-3-3ζ-labeled gold particles, indicating that both proteins were present in the filaments (Figure 6D). Compared to that of the ribbonlike filaments, the periodicity of PHF-like filaments was much smaller. While ribbonlike filaments displayed a flat surface, PHF-like filaments appeared to be twisted and ropelike. Thus, after incubation for 96 h, tau formed double-stranded, twisted filaments that resembled the PHFs of AD brain.[4,5]

Effect of Phosphorylation on 14-3-3ζ-Induced Tau Aggregation. PHFs are composed of phosphorylated tau.[2,27] To determine how phosphorylation affects tau aggregation, phosphorylated tau and nonphosphorylated tau were incubated for various time periods of time with 14-3-3ζ or the GST control. Samples were analyzed via a sedimentation assay for aggregation. As expected, tau incubated with GST did not aggregate (Figure 7A,C). Likewise, phosphorylated tau did not form any significant aggregation when incubated alone (data not shown) or with GST (Figure 7B,C). However, both tau and phosphorylated tau incubated with 14-3-3ζ showed an increased amount of aggregation in an incubation time-dependent manner (Figure 7A–C). More importantly, the relative aggregated amounts of both phosphorylated and nonphosphorylated tau were very similar at all time points (Figure 7C). These data indicate that under our experimental conditions, phosphorylation does not affect 14-3-3ζ-induced tau aggregation *in vitro*.

DISCUSSION

Abundant fibrillar tau in the affected brain regions is one of the most conspicuous features of a family of neurological disorders called tauopathies, which include AD, Picks disease, frontotemporal dementia and Parkinsonism linked to chromosome 17 (FTDP-17), corticobasal degeneration, and progressive supranuclear palsy.[1] Mutations have been observed in the familial type of FTDP-17.[30] These mutations promote tau fibrillization *in vitro* and in animal models.[1,31] So far, no AD-specific tau mutation has been observed in the human population, and it is not known what causes tau fibrillization in AD.

14-3-3ζ was reported to be present in NFT lesions from AD brain in a number of previous studies.[9−11] In addition, a study that examined the expressions of a variety of stress-related genes has reported that the expression of 14-3-3ζ was most significantly upregulated in AD brain and correlated with the severity of the disease.[11] A number of subsequent studies have shown that 14-3-3ζ binds to tau and promotes tau aggregation and/or tau phosphorylation.[2,8,13−21] The biochemical nature of the association of 14-3-3ζ within NFTs and the pathological significance of the interaction of 14-3-3ζ with tau have remained undetermined.

NFTs, in addition to tau, contain a number of other proteins. Therefore, to determine the biochemical mechanism of the association of 14-3-3ζ in PHFs, we purified PHFs from three

dx.doi.org/10.1021/bi400442d | *Biochemistry* 2013, 52, 6445−6455

pathologically well-characterized autopsied brains and analyzed 14-3-3ζ. We found that from each brain extract, 14-3-3ζ is copurified and co-immunoprecipitates with tau from the partially purified PHFs. Our data indicate that 14-3-3ζ is bound to tau within the PHFs.

14-3-3ζ is primarily a phosphoserine-binding protein.[8] However, 14-3-3ζ also binds to a number of target proteins that are phosphorylated at Thr residues or that are not phosphorylated at all.[8] PHF-tau is phosphorylated at a number of both Ser and Thr residues. Because of the biochemical nature of PHFs, it was not possible for us to determine if 14-3-3ζ is bound to any specific phosphorylated residue or if the interaction is independent of tau phosphorylation. However, both nonphosphorylated tau and phosphorylated tau specifically bind to GST-14-3-3ζ (Figure 2). When incubated *in vitro*, nonphosphorylated tau binds and forms PHF-like filaments (Figures 5 and 6). These data together indicate that tau phosphorylation is not required for 14-3-3ζ to bind to tau and associate with NFTs of AD brain.

Tau in the normal brain is a highly soluble protein without any ordered structure.[32] In contrast, tau in the AD brain is insoluble and displays a characteristic paired helical morphology.[32] Morphometric analysis has shown that tau, in AD brain, first forms amorphous aggregates in pretangle neurons.[33] These amorphous aggregates become fibrillar as the disease progresses. EM studies have determined that NFTs from AD brain contain two types of tau filaments: straight filaments and PHFs.[3] Both straight filaments and PHFs are coated with aggregated, amorphous tau, leaving a fuzzy image under the electron microscope.[3,6,7] In addition, when treated with alkali, PHFs untwist and form ribbonlike structures that have a periodicity much larger than that of the PHFs.[4] It is not known how these various morphological structures are formed or how they are related.

Tau forms amorphous aggregates, single-stranded filaments, ribbonlike filaments, and PHF-like filaments when incubated with 14-3-3ζ *in vitro* (Figures 5 and 6). These filaments display striking morphological similarities with the corresponding filaments of AD brain. The widths of the straight filaments found in AD brain[3] and the 14-3-3ζ-induced straight filaments are ∼15 and 18 nm, respectively (Figure 6). PHFs of AD brain display a width of 10−15 nm at the crossover and 27−35 nm at the loop, with a periodicity of ∼80 nm.[4,5] PHF-like filaments formed in the presence of 14-3-3ζ, on the other hand, have a width of ∼18 nm at the crossover and 27.9 nm at the loop, with a periodicity of ∼285 nm. Importantly, amorphous aggregated tau is the first ultrastructure formed when tau is incubated with 14-3-3ζ (Figure 5A−C). With an increased incubation time, these amorphous aggregates grow, become larger in size, and attach to single-stranded filaments (Figure 5D). Upon further incubation, the size of the amorphous aggregates on the filaments is reduced (Figure 5E), and double-stranded, ribbonlike filaments as well as PHF-like filaments appear (Figure 6A). While amorphous aggregates are extensively labeled with both gold-labeled anti-tau and anti-14-3-3ζ antibodies, all of the fibrillar structures subsequently formed are decorated less extensively (Figures 5 and 6), indicating that a significant number of epitopes that are recognized by the anti-tau and anti-14-3-3ζ antibodies that are exposed in the amorphous form become masked during the transformation of amorphous tau to its fibrillar structure. It is possible that during the progression of AD, tau first forms amorphous aggregates that become progressively larger, which then transform into single-stranded filaments. The single-stranded filaments then attach laterally to form ribbonlike, double-stranded filaments, and finally, the ribbonlike filaments twist, undergo a reduction in periodicity, and become PHFs. As indicated above, PHF-like filaments formed in the presence of 14-3-3ζ have a periodicity larger than the periodicity of those of AD brain. It is possible that PHF-like filaments may have to twist further to acquire the morphology of the PHFs found in AD.

PHFs are composed of hyperphosphorylated tau.[27] However, nonphosphorylated tau fibrillizes when incubated with heparin or α-synuclein.[25,28,29,34] Consistent with these reports, we also observed that when tau is incubated with 14-3-3ζ, it aggregates and forms PHF-like filaments (Figure 6). In addition, when incubated with 14-3-3ζ, phosphorylated tau also aggregates in a manner similar to that of nonphosphorylated tau (Figure 7). Together, these studies indicate that phosphorylation alone does not cause tau fibrillization, and tau phosphorylation is not required for tau aggregation. However, although not quantified in this study, the relative amount of 14-3-3ζ compared to the amount of tau within the PHFs is significantly smaller. *In vitro*, tau fibrillizes when incubated with an equimolar amount of 14-3-3ζ (Figure 4). These data suggest that only a fraction of tau fibrillization in AD brain is caused by 14-3-3ζ. A number of other factors such as heparin, α-synuclein, polyanions, and nucleic acids also cause tau fibrillization *in vitro*.[25,28,29,34,35] Tau phosphorylation, therefore, may influence tau fibrillization by any of these factors.

Sadik et al. determined that tau has two independent 14-3-3ζ binding sites: the microtubule-binding region and phosphorylated Ser^{214}.[18] Because 14-3-3ζ has a higher affinity for phosphorylated Ser^{214}, it binds to the microtubule-binding region only when tau is not phosphorylated at Ser^{214}.[18] Moreover, Sadik et al.[18] and Hernandez et al.[15] demonstrated that only binding of 14-3-3ζ to the microtubule-binding region causes tau aggregation. Phosphorylation at Ser^{214}, on the other hand, inhibits 14-3-3ζ-induced tau aggregation by binding 14-3-3ζ and, thus, preventing it from binding to the microtubule-binding region.[18]

In this study, we showed that phosphorylated tau aggregates in a manner similar to that of nonphosphorylated tau when incubated with 14-3-3ζ. Our data indicate that phosphorylation neither inhibits nor promotes 14-3-3ζ-induced tau aggregation and appear to contrast with the results of Sadik et al.[18] and Hernandez et al.[15] However, tau in the brain is phosphorylated at a number of sites by different kinases. Sadik et al.[18] and Hernandez et al.[15] used tau phosphorylated by PKA at Ser^{214}. Tau used in the study described here was phosphorylated to 7.9 mol of phosphates/mol of tau by kinases of rat brain extract, which contains several kinases, including PKA, and was very likely phosphorylated at a number of sites, including Ser^{214}. It is possible that phosphorylation at any of the other sites may inhibit the binding of 14-3-3ζ to phosphorylated Ser^{214} and neutralizes the effect of Ser^{214} phosphorylation on tau binding and aggregation. More studies will be required to fully determine the role of tau phosphorylation in 14-3-3ζ-induced tau aggregation.

■ ASSOCIATED CONTENT

Supporting Information

Figures 1−4. This material is available free of charge via the Internet at http://pubs.acs.org.

AUTHOR INFORMATION

Corresponding Author

*Lady Davis Institute for Medical Research, Jewish General Hospital, 3755 Côte-Sainte-Catherine Rd., Montreal, Quebec, Canada H3T 1E2. Telephone: (514) 340-8222, ext. 4866. Fax: (514) 340-7502. E-mail: hemant.paudel@mcgill.ca.

Author Contributions

H.Y.Q. and T.L. contributed equally to this work.

Funding

This work was supported by grants from Canadian Institute for Health Research and the Alzheimer's Society of Canada. R.M. and C.M.C. are recipients of Ph.D. fellowships from the Alzheimer's Society of Canada.

Notes

The authors declare no competing financial interest.

ABBREVIATIONS

AD, Alzheimer's disease; EM, electron microscopy; NFT, neurofibrillary tangle; PHF, paired helical filament; SE, standard error.

REFERENCES

(1) Brunden, K. R., Trojanowski, J. Q., and Lee, V. M. (2009) Advances in tau-focused drug discovery for Alzheimer's disease and related tauopathies. *Nat. Rev. Drug Discovery 8*, 783−793.

(2) Avila, J., Lucas, J. J., Perez, M., and Hernandez, F. (2004) Role of tau protein in both physiological and pathological conditions. *Physiol. Rev. 84*, 361−384.

(3) Crowther, R. A. (1991) Straight and paired helical filaments in Alzheimer disease have a common structural unit. *Proc. Natl. Acad. Sci. U.S.A. 88*, 2288−2292.

(4) Wischik, C. M., Crowther, R. A., Stewart, M., and Roth, M. (1985) Subunit structure of paired helical filaments in Alzheimer's disease. *J. Cell Biol. 100*, 1905−1912.

(5) Crowther, R. A., and Wischik, C. M. (1985) Image reconstruction of the Alzheimer paired helical filament. *EMBO J. 4*, 3661−3665.

(6) Wischik, C. M., Novak, M., Thogersen, H. C., Edwards, P. C., Runswick, M. J., Jakes, R., Walker, J. E., Milstein, C., Roth, M., and Klug, A. (1988) Isolation of a fragment of tau derived from the core of the paired helical filament of Alzheimer disease. *Proc. Natl. Acad. Sci. U.S.A. 85*, 4506−4510.

(7) Wischik, C. M., Novak, M., Edwards, P. C., Klug, A., Tichelaar, W., and Crowther, R. A. (1988) Structural characterization of the core of the paired helical filament of Alzheimer disease. *Proc. Natl. Acad. Sci. U.S.A. 85*, 4884−4888.

(8) Berg, D., Holzmann, C., and Riess, O. (2003) 14-3-3 proteins in the nervous system. *Nat. Rev. Neurosci. 4*, 752−762.

(9) Layfield, R., Fergusson, J., Aitken, A., Lowe, J., Landon, M., and Mayer, R. J. (1996) Neurofibrillary tangles of Alzheimer's disease brains contain 14.3-3 proteins. *Neurosci. Lett. 209*, 57−60.

(10) Umahara, T., Uchihara, T., Tsuchiya, K., Nakamura, A., Iwamoto, T., Ikeda, K., and Takasaki, M. (2004) 14-3-3 proteins and ζ isoform containing neurofibrillary tangles in patients with Alzheimer's disease. *Acta Neuropathol. 108*, 279−286.

(11) Soulie, C., Nicole, A., Delacourte, A., and Ceballos-Picot, I. (2004) Examination of stress-related genes in human temporal versus occipital cortex in the course of neurodegeneration: Involvement of 14-3-3ζ in this dynamic process. *Neurosci. Lett. 365*, 1−5.

(12) Agarwal-Mawal, A., Qureshi, H. Y., Cafferty, P. W., Yuan, Z., Han, D., Lin, R., and Paudel, H. K. (2003) 14-3-3 connects glycogen synthase kinase-3β to tau within a brain microtubule-associated tau phosphorylation complex. *J. Biol. Chem. 278*, 12722−12728.

(13) Chun, J., Kwon, T., Lee, E. J., Kim, C. H., Han, Y. S., Hong, S. K., Hyun, S., and Kang, S. S. (2004) 14-3-3 Protein mediates phosphorylation of microtubule-associated protein tau by serum- and glucocorticoid-induced protein kinase 1. *Mol. Cells 18*, 360−368.

(14) Hashiguchi, M., Sobue, K., and Paudel, H. K. (2000) 14-3-3ζ is an effector of tau protein phosphorylation. *J. Biol. Chem. 275*, 25247−25254.

(15) Hernandez, F., Cuadros, R., and Avila, J. (2004) Zeta 14-3-3 protein favours the formation of human tau fibrillar polymers. *Neurosci. Lett. 357*, 143−146.

(16) Li, T., and Paudel, H. K. (2007) 14-3-3ζ facilitates GSK3β-catalyzed tau phosphorylation in HEK-293 cells by a mechanism that requires phosphorylation of GSK3β on Ser9. *Neurosci. Lett. 414*, 203−208.

(17) Sadik, G., Tanaka, T., Kato, K., Yanagi, K., Kudo, T., and Takeda, M. (2009) Differential interaction and aggregation of 3-repeat and 4-repeat tau isoforms with 14-3-3ζ protein. *Biochem. Biophys. Res. Commun. 383*, 37−41.

(18) Sadik, G., Tanaka, T., Kato, K., Yamamori, H., Nessa, B. N., Morihara, T., and Takeda, M. (2009) Phosphorylation of tau at Ser214 mediates its interaction with 14-3-3 protein: Implications for the mechanism of tau aggregation. *J. Neurochem. 108*, 33−43.

(19) Sluchanko, N. N., Seit-Nebi, A. S., and Gusev, N. B. (2009) Phosphorylation of more than one site is required for tight interaction of human tau protein with 14-3-3ζ. *FEBS Lett. 583*, 2739−2742.

(20) Sluchanko, N. N., Seit-Nebi, A. S., and Gusev, N. B. (2009) Effect of phosphorylation on interaction of human tau protein with 14-3-3ζ. *Biochem. Biophys. Res. Commun. 379*, 990−994.

(21) Yuan, Z., Agarwal-Mawal, A., and Paudel, H. K. (2004) 14-3-3 binds to and mediates phosphorylation of microtubule-associated tau protein by Ser9-phosphorylated glycogen synthase kinase 3β in the brain. *J. Biol. Chem. 279*, 26105−26114.

(22) Ksiezak-Reding, H., and Yen, S. H. (1991) Structural stability of paired helical filaments requires microtubule-binding domains of tau: A model for self-association. *Neuron 6*, 717−728.

(23) Han, D., Qureshi, H. Y., Lu, Y., and Paudel, H. K. (2009) Familial FTDP-17 missense mutations inhibit microtubule assembly-promoting activity of tau by increasing phosphorylation at Ser202 in vitro. *J. Biol. Chem. 284*, 13422−13433.

(24) Lu, Y., Li, T., Qureshi, H. Y., Han, D., and Paudel, H. K. (2011) Early growth response 1 (Egr-1) regulates phosphorylation of microtubule-associated protein tau in mammalian brain. *J. Biol. Chem. 286*, 20569−20581.

(25) Giasson, B. I., Forman, M. S., Higuchi, M., Golbe, L. I., Graves, C. L., Kotzbauer, P. T., Trojanowski, J. Q., and Lee, V. M. (2003) Initiation and synergistic fibrillization of tau and α-synuclein. *Science 300*, 636−640.

(26) Qureshi, H. Y., and Paudel, H. K. (2011) Parkinsonian neurotoxin 1-methyl-4-phenyl-1,2,3,6-tetrahydropyridine (MPTP) and α-synuclein mutations promote Tau protein phosphorylation at Ser262 and destabilize microtubule cytoskeleton in vitro. *J. Biol. Chem. 286*, 5055−5068.

(27) Lee, V. M., Balin, B. J., Otvos, L., Jr., and Trojanowski, J. Q. (1991) A68: A major subunit of paired helical filaments and derivatized forms of normal tau. *Science 251*, 675−678.

(28) Goedert, M., Jakes, R., Spillantini, M. G., Hasegawa, M., Smith, M. J., and Crowther, R. A. (1996) Assembly of microtubule-associated protein tau into Alzheimer-like filaments induced by sulphated glycosaminoglycans. *Nature 383*, 550−553.

(29) Paudel, H. K., and Li, W. (1999) Heparin-induced conformational change in microtubule-associated protein tau as detected by chemical cross-linking and phosphopeptide mapping. *J. Biol. Chem. 274*, 8029−8038.

(30) Hutton, M., Lendon, C. L., Rizzu, P., Baker, M., Froelich, S., Houlden, H., Pickering-Brown, S., Chakraverty, S., Isaacs, A., Grover, A., Hackett, J., Adamson, J., Lincoln, S., Dickson, D., Davies, P., Petersen, R. C., Stevens, M., de Graaff, E., Wauters, E., van Baren, J., Hillebrand, M., Joosse, M., Kwon, J. M., Nowotny, P., Che, L. K., Norton, J., Morris, J. C., Reed, L. A., Trojanowski, J., Basun, H., Lannfelt, L., Neystat, M., Fahn, S., Dark, F., Tannenberg, T., Dodd, P. R., Hayward, N., Kwok, J. B., Schofield, P. R., Andreadis, A., Snowden, J., Craufurd, D., Neary, D., Owen, F., Oostra, B. A., Hardy, J., Goate, A., van Swieten, J., Mann, D., Lynch, T., and Heutink, P. (1998)

Association of missense and 5′-splice-site mutations in tau with the inherited dementia FTDP-17. *Nature 393*, 702−705.
(31) McGowan, E., Eriksen, J., and Hutton, M. (2006) A decade of modeling Alzheimer's disease in transgenic mice. *Trends Genet. 22*, 281−289.
(32) Lee, V. M., Goedert, M., and Trojanowski, J. Q. (2001) Neurodegenerative tauopathies. *Annu. Rev. Neurosci. 24*, 1121−1159.
(33) Galvan, M., David, J. P., Delacourte, A., Luna, J., and Mena, R. (2001) Sequence of neurofibrillary changes in aging and Alzheimer's disease: A confocal study with phospho-tau antibody, AD2. *J. Alzheimer's Dis. 3*, 417−425.
(34) Friedhoff, P., Schneider, A., Mandelkow, E. M., and Mandelkow, E. (1998) Rapid assembly of Alzheimer-like paired helical filaments from microtubule-associated protein tau monitored by fluorescence in solution. *Biochemistry 37*, 10223−10230.
(35) Konno, T., Oiki, S., Hasegawa, K., and Naiki, H. (2004) Anionic contribution for fibrous maturation of protofibrillar assemblies of the human tau repeat domain in a fluoroalcohol solution. *Biochemistry 43*, 13613−13620.